

# Origin of the second peak in the cross section of the $K^+\Lambda$ photoproduction

T. Mart and M. J. Kholili

*Departemen Fisika, FMIPA, Universitas Indonesia, Depok 16424, Indonesia*

(Dated: August 15, 2012)

## Abstract

By using a covariant isobar model and the latest experimental data we have analyzed the role of the  $P_{13}(1900)$  and  $D_{13}(2080)$  resonances in the kaon photoproduction process  $\gamma p \rightarrow K^+\Lambda$ . Special attention has been paid to the region where the second peak in the cross section is located, i.e. at total c.m. energies around 1.9 GeV. It is found that this peak originates mostly from the  $P_{13}(1900)$  resonance contribution. Although the contribution of the  $D_{13}(2080)$  resonance is not negligible, it is much smaller than that of the  $P_{13}(1900)$  state. Our finding confirms that the  $P_{13}(1900)$  resonance is also important in explaining the beam-recoil double polarization data  $C_x$  and  $C_z$ , provided that the mass and the width of this resonance are 1871 and 131 MeV, respectively.

PACS numbers: 13.60.Le, 25.20.Lj, 14.20.Gk

In 1998 the SAPHIR Collaboration observed for the first time a structure in the cross section of the  $\gamma p \rightarrow K^+ \Lambda$  process at a total c.m. energy  $W \approx 1.9$  GeV [1]. This structure was analyzed and interpreted as evidence for a “missing”  $D_{13}(1895)$  resonance [2] in the model called Kaon-Maid [3]. In spite of the fact that the inclusion of this resonance significantly improves the agreement between model predictions and experimental data, different interpretations have been also proposed [4, 5]. Nevertheless, despite considerable efforts devoted to settle this issue, there has been no solid answer to the question: which resonance or mechanism is responsible for this structure?

Armed with the new generation of kaon photoproduction data from the CLAS [7, 8], LEPS [9, 10] and GRAAL [11, 12] Collaborations, especially the double polarization  $C_x$  and  $C_z$  data from CLAS [8], the Bonn-Gatchina group reported the result of their coupled-channels partial waves analysis, that the structure should come from the contribution of the  $P_{13}(1900)$  resonance [6]. To our knowledge, the possibility of the  $P_{13}(1900)$  resonance as the origin of this structure was first pointed out in Ref. [2]. Nevertheless, it was ruled out because the extracted decay width did not agree with the prediction of the constituent quark model [13]. The role of this resonance was also briefly discussed in Refs. [14–16] and finally in Refs. [6, 17]. Since most analyses were performed in the framework of partial waves, it is therefore important to check this finding using the same tool as in Kaon-Maid, so that a comparison with Kaon-Maid can be made under the same conditions. Moreover, more precise experimental data [19] have been just made available after the Bonn-Gatchina report [6] appeared. Thus, we believe that a more accurate analysis could be expected.

To this end, we consider the standard nucleon resonances in the Particle Data Group (PDG) listing [20] which have masses between the  $K^+ \Lambda$  threshold (1.609 GeV) and 2.2 GeV, the same energy range considered in the Kaon-Maid analysis [2]. To simplify the analysis, as well as to make a fair comparison with Kaon-Maid, we limit the resonance spin only up to  $3/2$ . Furthermore, we also include the  $P_{11}(1840)$  state, which was found to be important in the photoproduction of  $K^+ \Lambda$ ,  $K^+ \Sigma^0$ , and  $K^0 \Sigma^+$  [17].

Our covariant isobar model is constructed from the appropriate Feynman diagrams consisting of the background and resonance terms with hadronic form factors inserted in hadronic vertices [18]. The background terms consist of the standard  $s$ -,  $u$ -, and  $t$ -channel Born terms along with the  $K^{*+}(892)$  and  $K_1(1270)$   $t$ -channel vector mesons. Two hyperon resonances that have been found to be important in reducing the divergence of the Born

terms at high energies [4], the  $S_{01}(1800)$  and  $P_{01}(1810)$ , are also included. For the resonance terms the model takes the  $S_{11}(1650)$ ,  $D_{13}(1700)$ ,  $P_{11}(1710)$ ,  $P_{13}(1720)$ ,  $P_{11}(1840)$ ,  $P_{13}(1900)$ ,  $D_{13}(2080)$ ,  $S_{11}(2090)$ , and  $P_{11}(2100)$  nucleon resonances into account. Their coupling constants were determined from fitting to a database consisting of differential cross section  $d\sigma/d\Omega$  [7, 9, 10, 19], recoil polarization  $P$  [7, 11], beam-recoil double polarization  $C_x, C_z$  [8] and  $O_{x'}, O_{z'}$  [12], as well as photon  $\Sigma$  and target  $T$  asymmetries [11] data. Thus, our present database consists of 3566 data points, whereas Kaon-Maid was only fitted to 319 data points [1].

To investigate the role of the  $D_{13}(2080)$  and  $P_{13}(1900)$  resonances in the  $\gamma p \rightarrow K^+ \Lambda$  process, we perform two different fits. In the first fit we fix the mass and width of the

TABLE I: Parameters of three important resonances obtained from fitting to the kaon photoproduction data in models A and B compared to those obtained from refitting Kaon-Maid, i.e. models A1 and B1. Numerical values printed with italic fonts indicate that the corresponding parameters are fixed during the fitting process.

Parameter	Present work		Kaon-Maid	
	A	B	A1	B1
$m_{D_{13}(2080)}$ (MeV)	1886	<i>2080</i>	1976	<i>2080</i>
$\Gamma_{D_{13}(2080)}$ (MeV)	244	<i>450</i>	736	<i>450</i>
$G_{D_{13}(2080)}^{(1)}$	-0.176	0.098	0.809	0.325
$G_{D_{13}(2080)}^{(2)}$	-0.085	0.015	0.726	0.244
$m_{P_{13}(1900)}$ (MeV)	<i>1900</i>	1871	<i>1900</i>	1954
$\Gamma_{P_{13}(1900)}$ (MeV)	<i>180</i>	131	<i>180</i>	123
$G_{P_{13}(1900)}^{(1)}$	-0.012	0.009	0.026	-0.025
$G_{P_{13}(1900)}^{(2)}$	-0.326	-0.203	0.038	-0.266
$m_{P_{11}(1840)}$ (MeV)	1952	1843	-	-
$\Gamma_{P_{11}(1840)}$ (MeV)	413	311	-	-
$g_{P_{11}(1840)}$	0.583	0.661	-	-
$N_{\text{data}}$	3566	3566	319	319
$\chi^2/N_{\text{dof}}$	2.57	2.68	2.42	3.12

$P_{13}(1900)$  resonance to their PDG values [20], i.e. 1900 and 180 MeV, respectively, whereas the mass and width of the  $D_{13}(2080)$  state are taken as free parameters. In the second fit, the mass and width of the  $P_{13}(1900)$  resonance are considered as free parameters, whereas those of the  $D_{13}(2080)$  state are fixed to the PDG values, i.e., 2080 and 450 MeV, respectively. For the sake of brevity, the first (second) fit will be called Model A (B). In all fits the mass and width of the  $P_{11}(1840)$  resonance are taken as free parameters.

Table I shows the parameters of three most important resonances extracted from the fitting process. Obviously, the fitted  $D_{13}$  and  $P_{13}$  masses tend to have values around 1900 MeV. This result might indicate that both  $D_{13}$  and  $P_{13}$  states could significantly contribute in both models. We note that when we exclude the  $P_{13}(1900)$  resonance the best  $\chi^2/N_{\text{dof}}$  obtained is 3.52, which is significantly larger than that obtained from both models.

It has been found that the  $P_{13}(1900)$  resonance is quite important in reproducing the  $C_x$  and  $C_z$  data [6]. In the present analysis we found that without this resonance, the contribution of the  $\chi^2$  from the  $C_x$  and  $C_z$  data to the total  $\chi^2$  is about 15%. Including this resonance in Model A (B) increases (decreases) this number to 16% (8%). The latter emphasizes the role of the  $P_{13}(1900)$  state in explaining the  $C_x$  and  $C_z$  data, provided that the mass and width of this state are taken as free parameters. Presumably, this is due to

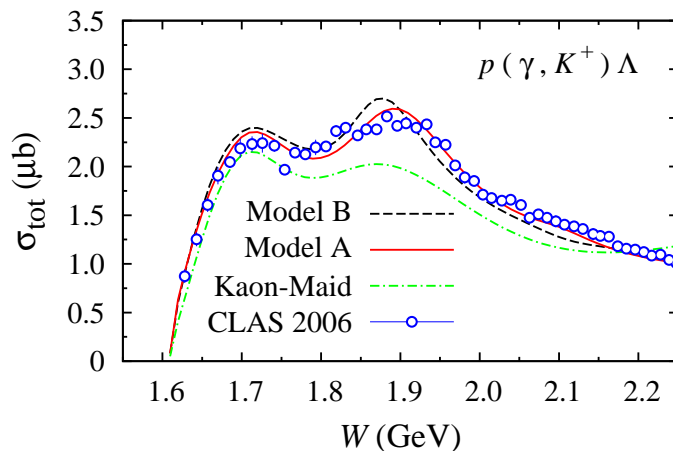


FIG. 1: (Color online) Total cross sections obtained by fitting the mass and width of the  $P_{13}(1900)$  (dashed line) and  $D_{13}(2080)$  (solid line) resonances compared with that obtained from Kaon-Maid (dash-dotted line) [3]. Experimental data are from the CLAS Collaboration [7] and were not used in the fitting process.

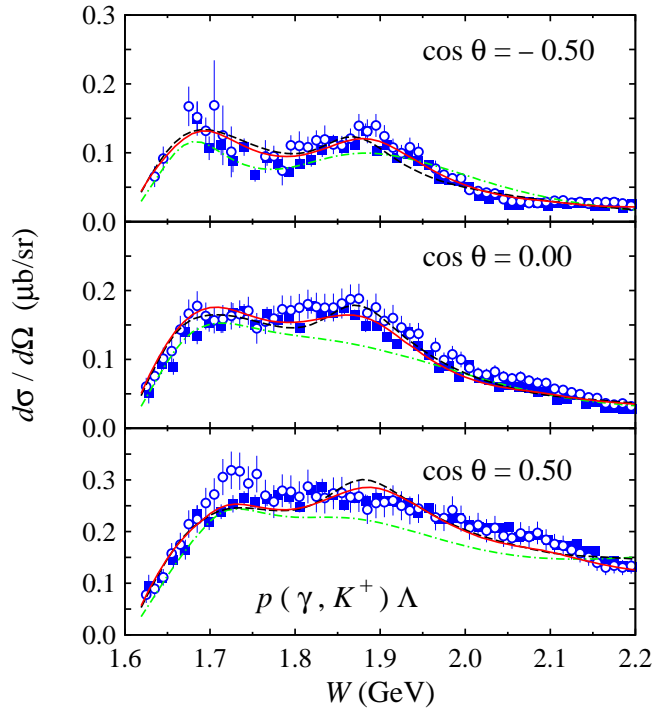


FIG. 2: (Color online) Same as Fig. 1, but for the differential cross sections sampled at three different kaon angles. Experimental data are from the CLAS Collaboration (solid squares [7] and open circles [19]).

the structure shown by the  $C_x$  and  $C_z$  data at  $W$  slightly below 1.9 GeV (see Fig. 5), which can be better explained by a  $P_{13}$  resonance rather than a  $D_{13}$  one.

However, it should be remembered that the increase of the  $\chi^2$  contribution after including the  $P_{13}(1900)$  resonance in Model A does not mean that the  $P_{13}(1900)$  is insignificant in explaining the the  $C_x$  and  $C_z$  data in this model, since the relative contribution discussed above refers to the total  $\chi^2$ , which is certainly smaller in Model A (i.e. 2.57 as compared to 3.52). This is elucidated by the individual  $\chi^2$  contributions shown in Fig. 6. Without the  $P_{13}(1900)$  resonance the  $C_x$  and  $C_z$  data contributes  $\chi^2 \approx 1832$  or equivalent to  $\chi^2/N \approx 9$ , where  $N = 202$  is the number of  $C_x$  and  $C_z$  data with total c.m. energies up to 2.2 GeV. Including this resonance in Model A (B) results in  $\chi^2 \approx 1414$  (756) or  $\chi^2/N \approx 7$  (4). Thus, one could conclude that in both models the role of the  $P_{13}(1900)$  state is found to be important in explaining the  $C_x$  and  $C_z$  data, especially in Model B. However, Fig. 6 also indicates that only the  $C_x$  and  $C_z$  data prefer Model B, in which the  $P_{13}$  mass is 1871 MeV.

Therefore, the second peak in the cross section (as well as other observables except the  $C_x$  and  $C_z$  ones) prefer a "different"  $P_{13}$  resonance with a mass of about 1900 MeV (Model A). This is understandable since the position of the peak is located around 1900 MeV. The result also explains the shift of the second peak calculated using Model B from the data, as is obviously seen in Figs. 1 and 7.

The need for two different  $P_{13}$  resonances in order to explain the experimental data around 1900 MeV could indicate the existence of two  $P_{13}$  resonances with masses around 1900 MeV. Indeed, in their recent study the Bonn-Gatchina group [6] found two poles around 1900 MeV, as will be discussed below.

The performance of the two models in explaining experimental data is shown in Figs. 1–5, where we also display predictions of Kaon-Maid for comparison. The underprediction of Kaon-Maid in both total and differential cross sections is understandable, since the SAPHIR 1998 cross sections [1] are smaller than the CLAS ones [7], especially at the second peak around 1.9 GeV. The better agreement of Model A with experimental data can be observed

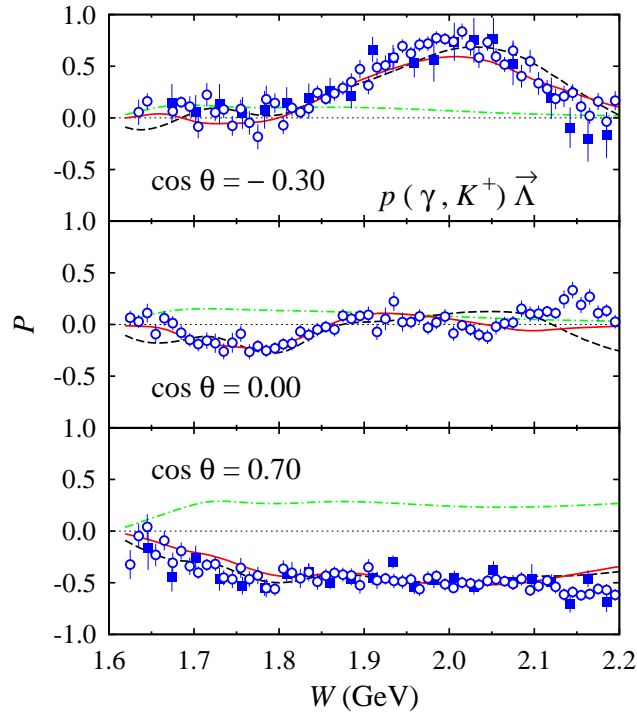


FIG. 3: (Color online) Same as Fig. 2, but for the recoil polarization observable  $P$ . Experimental data are from the CLAS Collaboration (solid squares [7] and open circles [19]).

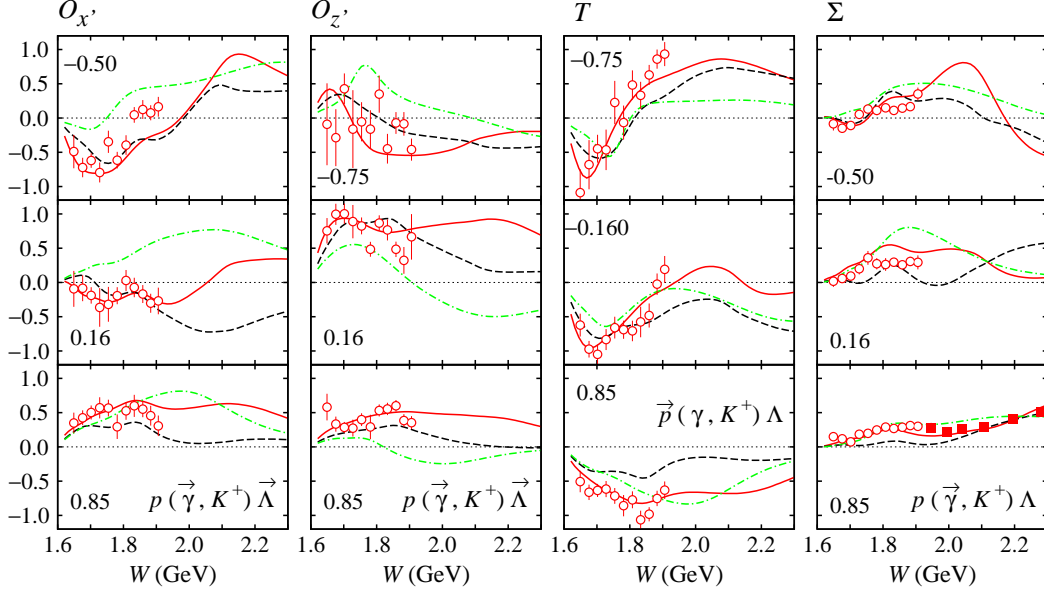


FIG. 4: (Color online) Same as Fig. 3, but for the beam-recoil double polarization observable  $O_{x'}$  and  $O_{z'}$  as well as the target  $T$  and beam  $\Sigma$  asymmetries. Experimental data are from the GRAAL [11, 12] (open circles) and LEPS Collaborations (solid circles) [9].

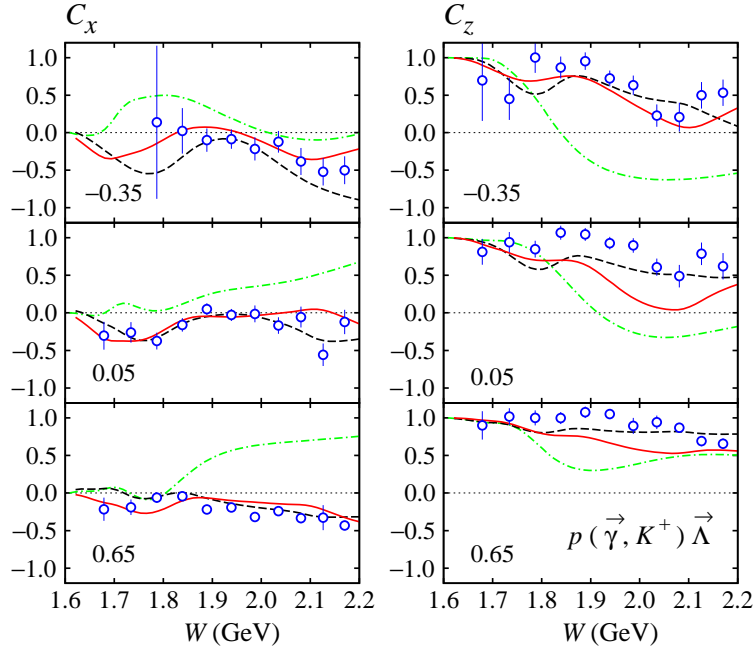


FIG. 5: (Color online) Same as Fig. 3, but for the beam-recoil double polarization observable  $C_x$  and  $C_z$ . Experimental data are from the CLAS Collaboration [8].

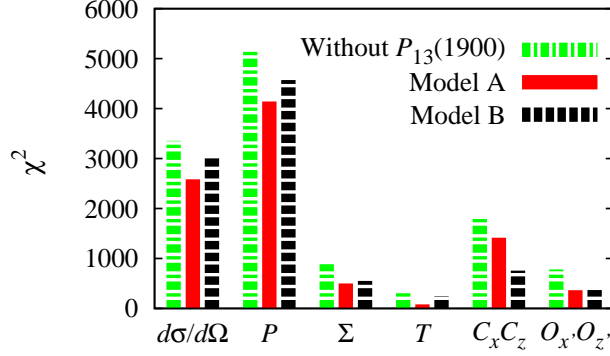


FIG. 6: (Color online) Individual  $\chi^2$  contributions from the differential cross section  $d\sigma/d\Omega$ , recoil polarization  $P$ , photon asymmetry  $\Sigma$ , target asymmetry  $T$ , and beam-recoil double polarization  $C_x, C_z$  and  $O_{x'}, O_{z'}$  data.

in all but  $C_x$  and  $C_z$  data, which is directly understood from the individual  $\chi^2$  contributions shown in Fig. 6. In fact, in both total and differential cross sections shown in Figs. 1 and 2 the second peak predicted by Model B seems to be shifted from experimental data, which might lead us to conclude that the second peak originates from the  $D_{13}$  contribution. However, this is not true.

To analyze the individual contributions of nucleon resonances to this process, we plot contributions of each resonance to the total cross section for both models in Fig. 7. Obviously, contributions of the  $S_{11}(1650)$  and  $P_{13}(1720)$  resonances explain the first peak of the cross section. It is also clear that the  $P_{11}(1710)$  resonance does not show up in this figure due to its small coupling to this process. This result corroborates our previous finding that uses the multipoles formalism to describe nucleon resonances [14]. The absence of the  $P_{11}(1710)$  resonance has been also pointed out in an extended partial-wave analysis of  $\pi N$  scattering data [21].

Obviously, Fig. 7 shows that the  $P_{13}(1900)$  resonance is responsible for the second peak in both models, whereas contribution of the  $D_{13}(2080)$  state at this point is relatively small. This finding is in good agreement with the claim of the Bonn-Gatchina group [6], which found two poles located at 1870 and 1950 MeV. Clearly, our finding corresponds to the first pole (see the second column of Table I). Furthermore, our result is also consistent with the previous coupled-channels study [15] and a very recent kaon photo- and electroproduction



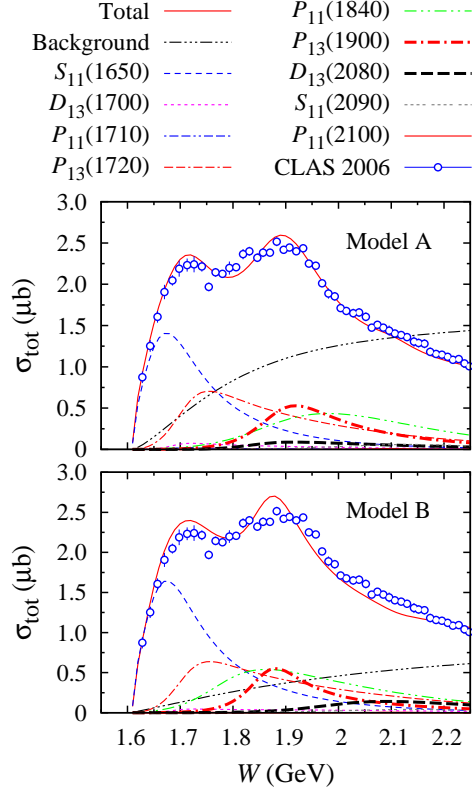


FIG. 7: (Color online) Contribution of the background and resonance amplitudes to the total cross section of the  $\gamma p \rightarrow K^+ \Lambda$  process when the mass and width of the  $D_{13}(2080)$  (Model A) or  $P_{13}(1900)$  (Model B) resonance are fitted. In both panels contributions of the  $D_{13}(2080)$  and  $P_{13}(1900)$  resonances are indicated by bold dashed and dash-dotted lines, respectively. Experimental data are from the CLAS Collaboration [7].

study based on a single-channel covariant isobar model [22]. As shown in Table II of Ref. [22], the magnitude of the  $P_{13}(1900)$  coupling constants is substantially larger than that of the  $D_{13}(2080)$  ones. This is valid not only for fitting to photoproduction data, but also for fitting to the combination of photo- and electroproduction data. Since the  $P_{13}$  and  $D_{13}$  resonances have different parities, we have checked the result of Ref. [22] explicitly and found that the contribution of the  $P_{13}$  state is much larger than that of the  $D_{13}$  state.

It also appears from Table I that both models yield different values of the  $P_{11}(1840)$  mass. Model B gives a better agreement with Ref. [17], whereas the extracted mass in Model A seems to be too high. Nevertheless, we also note that the later analysis from the Bonn-Gatchina group [23] yields a slightly larger mass range, i.e. 1850-1880 MeV.

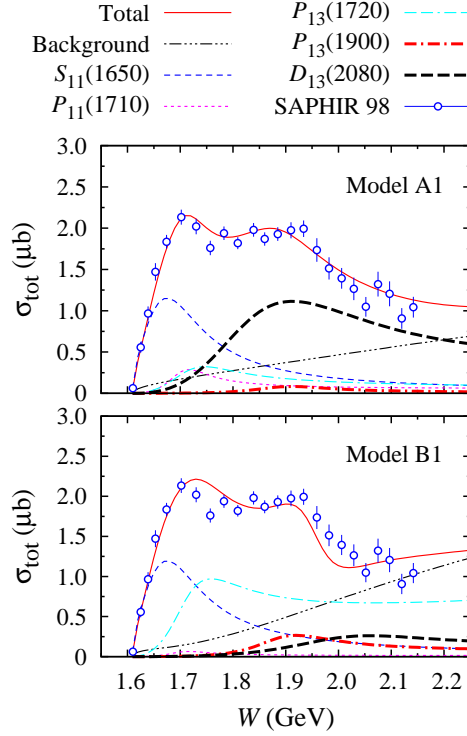


FIG. 8: (Color online) Same as Fig. 7, but for the refitted Kaon-Maid model. Note that the number of nucleon resonances used in the Kaon-Maid model is different from that of the present work. Experimental data are from the SAPHIR Collaboration [1].

If both  $P_{13}$  and  $D_{13}$  masses and widths are simultaneously fitted then we find a result almost similar to Model A, except the mass of the  $P_{13}$  is slightly shifted from 1900 MeV to 1891 MeV. Furthermore, it is also understood that the important role of the  $P_{13}(1900)$  in explaining the  $C_x$  and  $C_z$  data could be interpreted as simulating the final state interactions that are sensitive to the  $C_x$  and  $C_z$  observables. Therefore, although the present result corroborates the finding of the coupled-channels work of Ref. [6], a more thorough study using a dynamical coupled-channels approach, which fully takes into account the final state interaction effects, is still required.

The finding presented in this paper is obviously in contrast to the conclusion drawn more than a decade ago on the evidence of the  $D_{13}(1895)$  resonance [2]. Perhaps, it is interesting to ask why such a conclusion could be drawn. There are two possible answers to this question. The first one corresponds to the criteria of the "missing resonance." In Kaon-Maid the SAPHIR data were fitted to some possible states with masses around 1900 MeV

found in a constituent quark model [13], i.e., the  $S_{11}$ ,  $P_{11}$ ,  $P_{13}$ , and  $D_{13}$  resonances. The extracted masses of these states are found to be 1847, 1934, 1853, and 1895 MeV, with the corresponding  $\chi^2/N_{\text{dof}} = 2.70, 3.29, 3.15$ , and  $3.36$ , respectively. However, instead of using the  $\chi^2$ , the relevant "missing resonance" was determined by matching the corresponding decay width, which can be directly calculated from the extracted coupling constants, with the prediction of the constituent quark model [13]. As a result, the  $D_{13}$  state was found to be the most relevant "missing resonance".

The second answer is related to experimental data. As discussed above, the use of the  $P_{13}$  "missing resonance" to describe the SAPHIR data results in  $\chi^2/N_{\text{dof}} = 3.15$ , which is substantially larger than the use of the  $S_{11}$  "missing resonance". This indicates that to produce the second peak the data prefer an  $S_{11}$  state rather than a  $P_{13}$  state. To further investigate the role of the  $P_{13}(1900)$  resonance in the Kaon-Maid model, we refit the original model, but including this state in addition to the  $D_{13}$  state in the fit, and using the same database as in the original model. The relevant extracted parameters are listed in the fourth and fifth columns of Table I, while the contributions of individual resonances are depicted in Fig. 8. The result indicates that if we allow the  $D_{13}$  mass to vary, while the  $P_{13}$  mass is fixed to 1900 MeV (model A1), then the  $D_{13}$  contribution will dominate the whole cross section and simultaneously build up the second peak. Contribution of the  $P_{13}(1900)$  state is found to be tiny. Such a result is clearly still consistent with Kaon-Maid results.

However, a different conclusion would be obtained if we kept the  $D_{13}$  mass fixed at 2080 MeV and varied the  $P_{13}$  mass in the fit (model B1). As shown in Fig. 8, contribution of the  $D_{13}$  state is strongly suppressed now, whereas contribution of the  $P_{13}$  state is only slightly increased. To produce the second peak, contributions of both resonances must be added by a larger background. As a result, the total cross section obtained using this method shows a substantial difference from the previous one, especially at  $W \approx 2.0$  GeV. Therefore, we may conclude that the SAPHIR 1998 data do not prefer a  $P_{13}$  state as a dominant contributor to the second peak in the cross section.

In conclusion we have analyzed the role of  $P_{13}(1900)$  and  $D_{13}(2080)$  resonances in the  $K^+\Lambda$  photoproduction off a proton, focusing on the second peak in the cross section as well as on the CLAS  $C_x$  and  $C_z$  data. We found that the peak originates mostly from the  $P_{13}(1900)$  resonance. In contrast to Kaon-Maid results, the contribution of the  $D_{13}(2080)$  is much smaller, even though its mass was fitted and found to be 1886 MeV, i.e., very close to

the position of second peak. The  $P_{13}$  resonance is also found to be important in reproducing the  $C_x$  and  $C_z$  data. The absence of the  $P_{13}(1900)$  contribution in Kaon-Maid is related to the SAPHIR 1998 data, since the corresponding second peak can be best explained by means of the  $D_{13}(2080)$  resonance. The present finding does not by any means reject the claim that the second peak could provide evidence for a  $D_{13}$  resonance with  $m \approx 1900$  MeV. It only shows that the evidence is weak.

This work has been supported in part by the University of Indonesia and the Competence Grant of the Indonesian Ministry of Education and Culture.

- 
- [1] M. Q. Tran *et al.* [SAPHIR Collaboration], Phys. Lett. B **445**, 20 (1998). References for older data can be found in the references of this paper.
  - [2] T. Mart and C. Bennhold, Phys. Rev. C **61**, 012201 (1999).
  - [3] Available at the Maid homepage <http://www.kph.uni-mainz.de/MAID/kaon/kaonmaid.html>. The published versions can be found in: Ref. [2]; T. Mart, Phys. Rev. C **62**, 038201 (2000); C. Bennhold, H. Haberzettl and T. Mart, arXiv:nucl-th/9909022.
  - [4] S. Janssen, J. Ryckebusch, W. Van Nispen, D. Debruyne and T. Van Cauteren, Eur. Phys. J. A **11**, 105 (2001)
  - [5] A. Martinez Torres, K. P. Khemchandani, U. G. Meissner and E. Oset, Eur. Phys. J. A **41**, 361 (2009).
  - [6] V. A. Nikonov, A. V. Anisovich, E. Klempt, A. V. Sarantsev and U. Thoma, Phys. Lett. B **662**, 245 (2008).
  - [7] R. Bradford *et al.* [CLAS Collaboration], Phys. Rev. C **73**, 035202 (2006).
  - [8] R. Bradford *et al.* [CLAS Collaboration], Phys. Rev. C **75**, 035205 (2007).
  - [9] M. Sumihama *et al.* [LEPS Collaboration], Phys. Rev. C **73**, 035214 (2006).
  - [10] K. Hicks *et al.* [LEPS Collaboration], Phys. Rev. C **76**, 042201 (2007).
  - [11] A. Lleres *et al.*, Eur. Phys. J. A **31**, 79 (2007).
  - [12] A. Lleres *et al.*, Eur. Phys. J. A **39**, 146 (2009).
  - [13] S. Capstick and W. Roberts, Phys. Rev. D **49**, 4570 (1994).
  - [14] T. Mart and A. Sulaksono, Phys. Rev. C **74**, 055203 (2006).
  - [15] B. Julia-Diaz, B. Saghai, T. S. H. Lee and F. Tabakin, Phys. Rev. C **73**, 055204 (2006).

- [16] S. Janssen, J. Ryckebusch, D. Debruyne and T. Van Cauteren, Phys. Rev. C **65**, 015201 (2001).
- [17] A. V. Sarantsev, V. A. Nikonov, A. V. Anisovich, E. Klempt and U. Thoma, Eur. Phys. J. A **25**, 441 (2005).
- [18] H. Haberzettl, C. Bennhold, T. Mart and T. Feuster, Phys. Rev. C **58**, 40 (1998).
- [19] M. E. McCracken *et al.* [CLAS Collaboration], Phys. Rev. C **81**, 025201 (2010).
- [20] K. Nakamura *et al.*, J. Phys. G **37**, 075021 (2010).
- [21] R. A. Arndt, W. J. Briscoe, I. I. Strakovsky and R. L. Workman, Phys. Rev. C **74**, 045205 (2006).
- [22] O. V. Maxwell, Phys. Rev. C **85**, 034611 (2012).
- [23] A. V. Anisovich, E. Klempt, V. A. Nikonov, A. V. Sarantsev, and U. Thoma, Eur. Phys. J. A **47**, 27 (2011).